



## Role of Formins in Actin Assembly: Nucleation and Barbed-End Association

David Pruyne, *et al.*  
*Science* **297**, 612 (2002);  
DOI: 10.1126/science.1072309

**The following resources related to this article are available online at [www.sciencemag.org](http://www.sciencemag.org) (this information is current as of January 29, 2007):**

**Updated information and services**, including high-resolution figures, can be found in the online version of this article at:

<http://www.sciencemag.org/cgi/content/full/297/5581/612>

**Supporting Online Material** can be found at:

<http://www.sciencemag.org/cgi/content/full/1072309/DC1>

A list of selected additional articles on the Science Web sites **related to this article** can be found at:

<http://www.sciencemag.org/cgi/content/full/297/5581/612#related-content>

This article **cites 30 articles**, 16 of which can be accessed for free:

<http://www.sciencemag.org/cgi/content/full/297/5581/612#otherarticles>

This article has been **cited by** 195 article(s) on the ISI Web of Science.

This article has been **cited by** 84 articles hosted by HighWire Press; see:

<http://www.sciencemag.org/cgi/content/full/297/5581/612#otherarticles>

This article appears in the following **subject collections**:

Cell Biology

[http://www.sciencemag.org/cgi/collection/cell\\_bio](http://www.sciencemag.org/cgi/collection/cell_bio)

Information about obtaining **reprints** of this article or about obtaining **permission to reproduce this article** in whole or in part can be found at:

<http://www.sciencemag.org/help/about/permissions.dtl>

# Role of Formins in Actin Assembly: Nucleation and Barbed-End Association

David Pruyne,<sup>1\*</sup> Marie Evangelista,<sup>2\*</sup> Changsong Yang,<sup>3</sup> Erfei Bi,<sup>4</sup> Sally Zigmond,<sup>3</sup> Anthony Bretscher,<sup>1†</sup> Charles Boone<sup>2,5†</sup>

Nucleation of branched actin filaments by the Arp2/3 complex is a conserved process in eukaryotic cells, yet the source of unbranched actin filaments has remained obscure. In yeast, formins stimulate assembly of actin cables independently of Arp2/3. Here, the conserved core of formin homology domains 1 and 2 of Bni1p (Bni1pFH1FH2) was found to nucleate unbranched actin filaments *in vitro*. Bni1pFH2 provided the minimal region sufficient for nucleation. Unique among actin nucleators, Bni1pFH1FH2 remained associated with the growing barbed ends of filaments. This combination of properties suggests a direct role for formins in regulating nucleation and polarization of unbranched filamentous actin structures.

Formins are cytoskeleton-organizing proteins present in fungi, plants, and animals that are implicated as effectors for Rho-type guanosine triphosphatases (GTPases) (1–3) in regulating cytokinesis, polarized growth, and stress fiber formation (4–6). Formins bear a proline-rich formin homology-1 (FH1) domain, which binds profilin and protein-protein interaction modules, such as SH3 and WW domains, and an adjacent FH2 domain of unknown function (Fig. 1A). In budding yeast, the formins Bni1p and Bnr1p drive the assembly of bundles of filaments called actin

cables (7, 8) that direct polarized growth and organelle segregation (9–13). Formin-dependent cable assembly occurs in the absence of a functional Arp2/3 actin nucleation complex (7, 14). In contrast, the cortical actin patches of yeast persist in the absence of formin function (7, 8) and require Arp2/3 to assemble and participate in endocytosis (14). Because ectopic expression of NH<sub>2</sub>-terminally truncated Bni1p—lacking the regulatory Rho-binding domain but containing the FH1, FH2, and a Bni1p-specific COOH-terminal extension (Bni1pFH1FH2COOH)—induces

massive filament assembly *in vivo* (2, 7), we set out to reconstitute formin-stimulated actin filament assembly *in vitro*.

Bacterially expressed glutathione-S-transferase (GST)–fusion protein containing Bni1pFH1FH2COOH (Fig. 1A, fig. S1) was sufficient to nucleate filaments of purified actin, as measured by increased fluorescence of pyrene-conjugated actin upon polymerization (Fig. 1B) (15). The ability of Bni1pFH1FH2COOH to induce filament assembly *in vivo* depends upon profilin (7). However, under these *in vitro* conditions, profilin partially inhibited, rather than enhanced, nucleation at concentrations sufficient to sequester most of the actin monomers (16), suggesting that profilin-actin is a less efficient substrate than free G-actin. Unlike the case for the Arp2/3 complex (17), preformed actin filaments did not enhance nucleation (16). Thus, formins may

<sup>1</sup>Department of Molecular Biology and Genetics, Cornell University, Ithaca, NY 14853, USA. <sup>2</sup>Department of Biology, Queen's University, Kingston, Ontario, K7L 3N6 Canada. <sup>3</sup>Biology Department, University of Pennsylvania, Philadelphia, PA 19104–6018, USA. <sup>4</sup>Department of Cell and Developmental Biology, University of Pennsylvania, Philadelphia, PA 19104, USA. <sup>5</sup>Banting and Best Department of Medical Research and Department of Molecular and Medical Genetics, University of Toronto, Toronto, Ontario, M5G 1L6 Canada.

\*These authors contributed equally to this work.

†To whom correspondence should be addressed. E-mail: apb5@cornell.edu (A.B.), charlie.boone@utoronto.ca (C.B.)

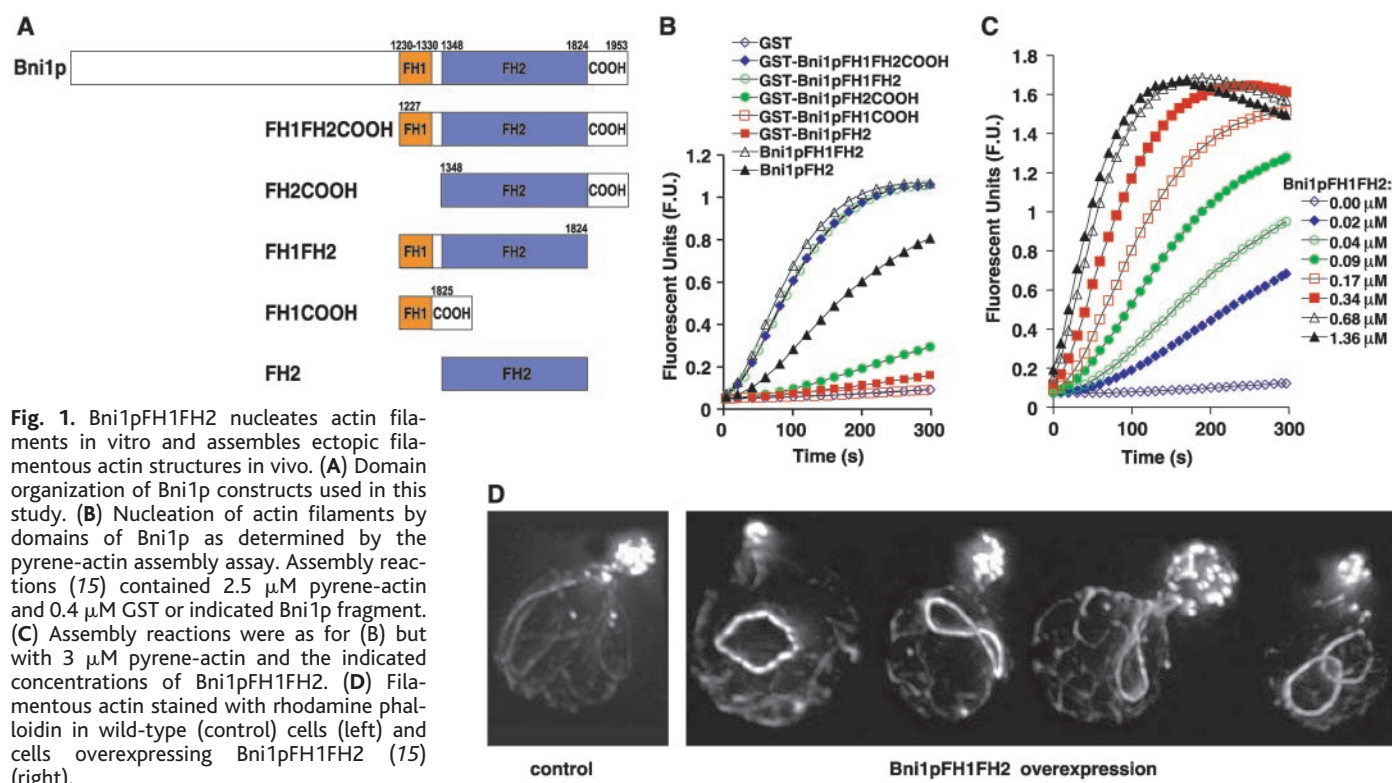


**Fig. 1.** Bni1pFH1FH2 nucleates actin filaments *in vitro* and assembles ectopic filamentous actin structures *in vivo*. (A) Domain organization of Bni1p constructs used in this study. (B) Nucleation of actin filaments by domains of Bni1p as determined by the pyrene-actin assembly assay. Assembly reactions (15) contained 2.5 μM pyrene-actin and 0.4 μM GST or indicated Bni1p fragment. (C) Assembly reactions were as for (B) but with 3 μM pyrene-actin and the indicated concentrations of Bni1pFH1FH2. (D) Filamentous actin stained with rhodamine phalloidin in wild-type (control) cells (left) and cells overexpressing Bni1pFH1FH2 (15) (right).

REPORTS

regulate actin filament assembly by nucleating filaments.

The FH2 domain was originally defined as a conserved ~100-residue sequence (18, 19); but the analysis of additional forms revealed that the similarity extends over ~500 amino acids (Fig. 1A) (6, 20). On the basis of this domain delineation, fragments of Bni1pFH1FH2COOH (Fig. 1A, fig. S1) were assessed for their ability to assemble actin

filaments in vitro by pyrene-actin polymerization assays, and in vivo by expression from the inducible *GAL1* promoter (15). Both GST-Bni1pFH1FH2 lacking the COOH-terminal extension and purified Bni1pFH1FH2 lacking the GST tag showed in vitro nucleating activity similar to that of GST-Bni1pFH1FH2COOH (Fig. 1B), indicating that neither the COOH-terminal extension nor the GST tag contributed to nucleation.

This nucleating activity was dose-dependent on Bni1pFH1FH2 (Fig. 1C). Deletion of the FH2 domain abolished nucleating activity, and deletion of the FH1 domain from GST-Bni1pFH1FH2 diminished its activity to ~10%; however, cleavage of GST to generate isolated FH2 restored nucleation to ~50% that of GST-Bni1pFH1FH2 (Fig. 1B). Ectopic expression in yeast of all constructs containing both FH1 and FH2 domains (15) were lethal and associated with the aberrant accumulation of actin cables (7) or ringlike filamentous actin structures (Fig. 1D), whereas expression of fragments lacking the FH1 or the FH2 had no effect (16). This requirement for the FH1 domain is consistent with an in vivo role for profilin in formin-mediated actin assembly (7). Thus, the FH2 domain is an actin nucleator, and its NH<sub>2</sub>-terminal context is important for its activity in vitro and in vivo.

The extent and rate of Bni1pFH1FH2-stimulated nucleation increased with the initial G-actin concentration (Fig. 2A) (15), with little or no nucleation within 5 min at or below 0.5 μM G-actin (16). To determine whether GST-Bni1pFH1FH2-induced assembly involved barbed-end growth, we compared the effects of cytochalasin B (CB), an inhibitor of barbed-end filament growth (21), on assembly from several different nucleators (15). Seeds of spectrin and actin, isolated from erythrocyte ghosts, assemble actin at both barbed and pointed ends (22). Isolated gelsolin (23) nucleates filaments in vitro that are capped at the barbed end and elongate exclusively from the pointed end (24). Spectrin-actin seeds, gelsolin-actin nuclei, and GST-Bni1pFH1FH2 were each incubated with 1.5 μM G-actin (a concentration favoring barbed- over pointed-end assembly ~10-fold) (25). As expected, CB substantially inhibited the growth of spectrin-actin seeds (89%) but not that of gelsolin-capped filaments (2%) (Fig. 2B). GST-Bni1pFH1FH2-stimulated filament growth was partially inhibited (63%), suggesting barbed-end growth of Bni1pFH1FH2-nucleated filaments or, alternatively, that the Bni1pFH1FH2 nucleation event was directly inhibited by CB (15).

To investigate whether Bni1pFH1FH2-induced nucleation was CB sensitive, we first examined the reversibility of CB-induced inhibition on elongation (15). Because the critical concentration for the pointed ends of actin filaments is ~0.5 μM G-actin (25), elongation of spectrin-actin seeds in 0.5 μM G-actin occurs only at the barbed end, a reaction completely inhibited by 2 μM CB (Fig. 2C). However, when seeds were preincubated with 2 μM CB and then diluted into 0.1 μM CB and 0.5 μM G-actin, elongation occurred with an efficiency similar to that of seeds incubated in 0.1 μM CB directly (Fig.

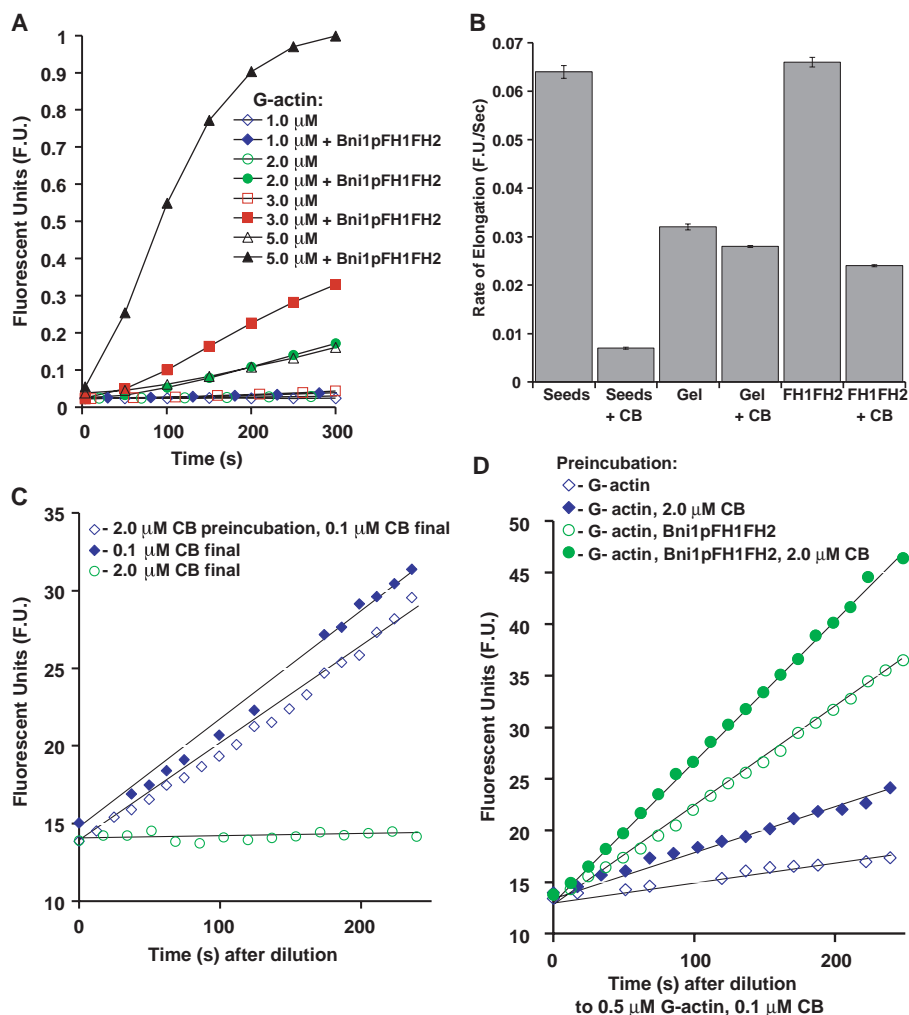


**Fig. 2.** Bni1pFH1FH2-induced actin assembly shows G-actin dose dependence, and elongation but not nucleation is cytochalasin B (CB) sensitive. (A) Indicated concentrations of G-actin were incubated with or without 90 nM Bni1pFH1FH2, and pyrene-actin assembly was followed (15). Each curve was normalized to the predicted end-point to compensate for differences in pyrene-actin concentrations. (B) GST-Bni1pFH1FH2 or preformed nuclei of spectrin-actin or gelsolin-actin were added to 1.5 μM pyrene-actin, and filament assembly was monitored in the absence or presence (+ CB) of 2 μM CB (15). CB-induced inhibition likely underestimates the extent of barbed-end growth during GST-Bni1pFH1FH2-stimulated assembly (15). (C) Inhibition of elongation by CB is reversible. Spectrin-actin seeds were preincubated with (open diamonds) or without (filled diamonds) 2 μM CB before dilution into 0.5 μM pyrene-actin without or with 0.1 μM CB, both giving a final concentration of 0.1 μM CB (15). Control samples (open circles) included 2 μM CB throughout the assembly reaction. (D) Bni1pFH1FH2-induced nucleation is not CB sensitive. G-actin (3 μM) was incubated for 3 min with 0.2 μM GST-Bni1pFH1FH2 in the presence (filled circles) or absence (open circles) of 2 μM CB before dilution into a final concentration of 0.1 μM CB as above (15). Controls preincubated 3 μM G-actin without GST-Bni1pFH1FH2 or CB (open diamonds) or preincubated 3 μM G-actin with 2 μM CB alone (filled diamonds). Preincubation with 2 μM CB slightly enhanced nucleation, perhaps by suppressing elongation and thereby retaining higher concentrations of G-actin available for nucleation (15).

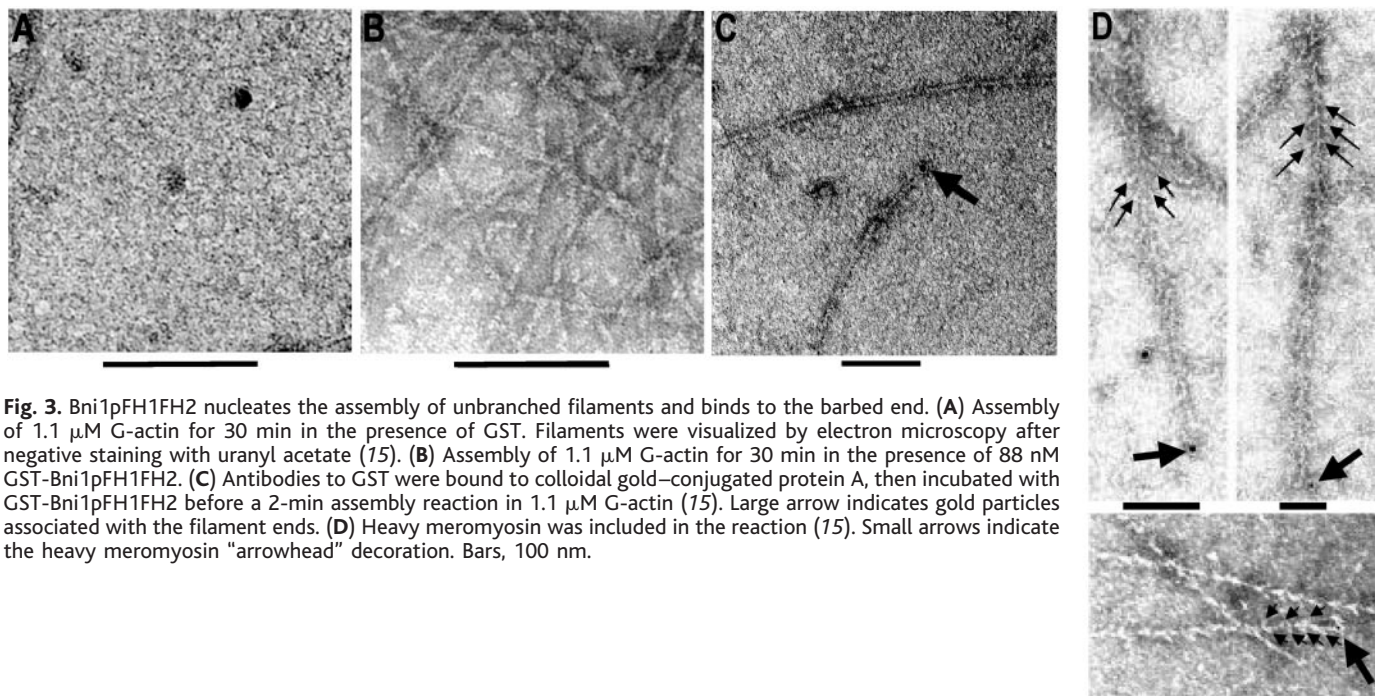
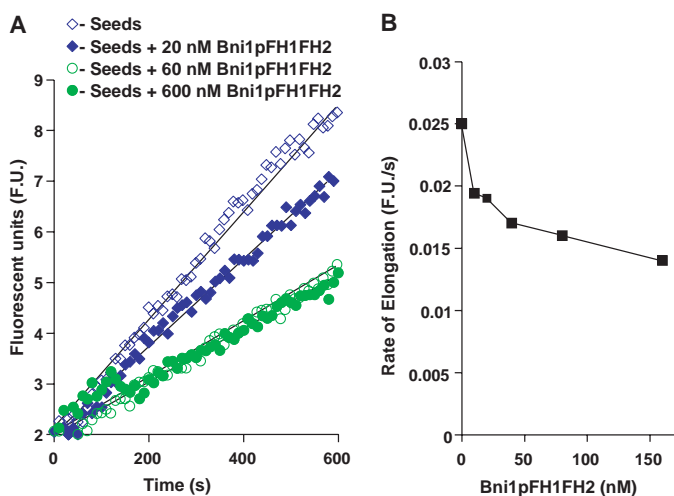


**Fig. 3.** Bni1pFH1FH2 nucleates the assembly of unbranched filaments and binds to the barbed end. (A) Assembly of 1.1  $\mu\text{M}$  G-actin for 30 min in the presence of GST. Filaments were visualized by electron microscopy after negative staining with uranyl acetate (15). (B) Assembly of 1.1  $\mu\text{M}$  G-actin for 30 min in the presence of 88 nM GST-Bni1pFH1FH2. (C) Antibodies to GST were bound to colloidal gold-conjugated protein A, then incubated with GST-Bni1pFH1FH2 before a 2-min assembly reaction in 1.1  $\mu\text{M}$  G-actin (15). Large arrow indicates gold particles associated with the filament ends. (D) Heavy meromyosin was included in the reaction (15). Small arrows indicate the heavy meromyosin "arrowhead" decoration. Bars, 100 nm.

**Fig. 4.** Bni1pFH1FH2 slows barbed-end elongation. (A) Spectrin-actin seeds (0.8 nM) were incubated with 0.5  $\mu\text{M}$  pyrene-actin, and the effect on elongation of the indicated concentration of GST-Bni1pFH1FH2 was assessed (15). Under these conditions, GST-Bni1pFH1FH2 did not nucleate assembly. (B) The calculated rates of actin assembly were plotted against GST-Bni1pFH1FH2 concentration, giving a maximum inhibition rate of  $\sim 50\%$  with a half-maximal inhibition  $K_d$  of 20 nM GST-Bni1pFH1FH2.



the polarity of the actin filaments, they were decorated with heavy meromyosin. We found a significant bias for the gold-labeled GST-Bni1pFH1FH2 fragment to label the barbed end (mean  $\pm$  SD, 83.5  $\pm$  3.0%) (Fig. 3D), whereas in the absence of the antibody the residual nonspecific labeling showed no predisposition (mean  $\pm$  SD, 49.3  $\pm$  4.6% barbed end). When the background level of end-labeling observed in the control was accounted for (15), all end-associated GST-Bni1pFH1FH2 appeared to reside at the barbed end.

The association of Bni1pFH1FH2 with the barbed end indicated it might also function as a capping protein. Proteins that cap barbed ends, such as villin (26), gelsolin (24), and CapZ (27), also show actin nucleating activity in vitro. We examined the effect of including increasing amounts of Bni1pFH1FH2 on the barbed-end growth of spectrin-actin seeds (15). GST-Bni1pFH1FH2 inhibited filament elongation in a dose-dependent manner (Fig. 4, A and B), but with a maximal inhibition of only  $\sim 50\%$ , even at the highest levels of GST-Bni1pFH1FH2 (600 nM), where  $\sim 95\%$  of the barbed ends were predicted to be associated with this fragment (16). The half-maximal inhibition indicated a dissociation constant ( $K_d$ ) of 20 nM GST-Bni1pFH1FH2 for the capping activity. This "partial" capping is in marked contrast to all other known barbed end-binding proteins, which abolish barbed-end elongation (24, 27). Rather, under physiological conditions, where the concentration of G-actin is expected to be low, Bni1pFH1FH2-nucleated filaments are predicted to grow exclusively from their barbed ends.

2C). Because dilution rapidly reversed CB-induced inhibition of elongation, we were able to test whether Bni1pFH1FH2-induced nucleation was CB sensitive (15). GST-Bni1pFH1FH2 was preincubated with 3  $\mu\text{M}$  G-actin to allow nucleation, either in the presence or absence of 2  $\mu\text{M}$  CB, and then the reactions were diluted to a final concentration of 0.1  $\mu\text{M}$  CB and 0.5  $\mu\text{M}$  G-actin, an actin concentration permitting barbed-end growth of formed nuclei but preventing new nucleation (Fig. 2D). In both cases, GST-Bni1pFH1FH2 stimulated nucleation as compared with actin alone. Thus, CB must have exerted its effects by inhibiting elongation, and Bni1pFH1FH2-induced filaments grew largely from the barbed end (15).

Examination of GST-Bni1pFH1FH2-stimulated structures by electron microscopy (15) revealed a profusion of long ( $>1$  to 2  $\mu\text{m}$ ), unbranched filaments (Fig. 3, A and B). To localize Bni1pFH1FH2 with assembling filaments, GST-Bni1pFH1FH2 was bound to colloidal gold-conjugated protein A via GST-specific antibody before dilution into purified 1.1  $\mu\text{M}$  G-actin. After 2 min of polymerization, a subset (mean  $\pm$  SD, 28  $\pm$  2.2%) of filaments had colloidal gold associated with one end (Fig. 3C), whereas controls lacking anti-GST showed a significantly lower fraction of end labeling (mean  $\pm$  SD, 3.0  $\pm$  2.2%). These findings raised the possibility that Bni1pFH1FH2 associates with a particular filament end. To visualize

Thus, the Bni1p FH2 domain is an actin nucleator with unique properties for polarizing growing filaments. In vitro, Bni1pFH1FH2 stimulates assembly of unbranched filaments and associates with their barbed ends, yet still permits barbed-end growth. In vivo, yeast formins direct assembly of actin cables (7, 8) that radiate from discrete regions of the growing cell cortex (28) where the formins are localized (2, 29–31). Unidirectional movements of a cable-dependent myosin-V indicate that cable filaments are oriented with their barbed ends directed toward the growing cortex (32), and in vivo actin cable dynamics have shown that cables assemble at these sites (33). Our observations suggest that Bni1p directly nucleates cable filaments and tethers them by their growing barbed ends, establishing their polarity. Conservation of this mechanism may explain the roles of formins in the assembly of unbranched filamentous actin arrays in other eukaryotes.

References and Notes

1. H. Kohno *et al.*, *EMBO J.* **15**, 6060 (1996).
2. M. Evangelista *et al.*, *Science* **276**, 118 (1997).
3. H. Imamura *et al.*, *EMBO J.* **16**, 2745 (1997).
4. A. J. Ridley, *Nature Cell Biol.* **1**, E64 (1999).
5. S. Wasserman, *Trends Cell Biol.* **8**, 111 (1998).
6. R. Zeller *et al.*, *Cell Tissue Res.* **296**, 85 (1999).
7. M. Evangelista, D. Pruyne, D. C. Amberg, C. Boone, A. Bretscher, *Nature Cell Biol.* **4**, 32 (2002).
8. I. Sagot, S. K. Klee, D. Pellman, *Nature Cell Biol.* **4**, 42 (2002).
9. D. W. Pruyne, D. H. Schott, A. Bretscher, *J. Cell Biol.* **143**, 1931 (1998).
10. K. L. Hill, N. L. Catlett, L. S. Weisman, *J. Cell Biol.* **135**, 1535 (1996).
11. C. L. Theesfeld, J. E. Irazoqui, K. Bloom, D. J. Lew, *J. Cell Biol.* **146**, 1019 (1999).
12. O. W. Rossanese *et al.*, *J. Cell Biol.* **153**, 47 (2001).
13. D. Hoepfner, M. van den Berg, P. Philippsen, H. F. Tabak, E. H. Hettema, *J. Cell Biol.* **155**, 979 (2001).
14. D. C. Winter, E. Y. Choe, R. Li, *Proc. Natl. Acad. Sci. U.S.A.* **96**, 7288 (1999).
15. The following supplementary materials are available on Science Online: a description of materials and methods and a note providing further discussion of the defects of CB on nucleation by GST-Bni1pFH1FH2, and fig. S1.
16. D. Pruyne *et al.*, data not shown.
17. L. M. Machesky *et al.*, *Proc. Natl. Acad. Sci. U.S.A.* **96**, 3739 (1999).
18. D. H. Castrillon, S. A. Wasserman, *Development* **120**, 3367 (1994).
19. S. Emmons *et al.*, *Genes Dev.* **9**, 2482 (1995).
20. The domain organization of Bni1p was based on the analysis of 75 formin orthologs accessed through the Pfam database of protein domains (<http://pfam.wustl.edu/index.html>).
21. S. MacLean-Fletcher, T. D. Pollard, *Cell* **20**, 329 (1980).
22. D. C. Lin, S. Lin, *Anal. Biochem.* **103**, 316 (1980).
23. J. A. Cooper *et al.*, *J. Cell Biol.* **104**, 491 (1987).
24. R. Tellam, C. Frieden, *Biochemistry* **21**, 3207 (1982).
25. T. D. Pollard, L. Blanchoin, R. D. Mullins, *Annu. Rev. Biophys. Biomol. Struct.* **29**, 545 (2000).
26. J. R. Glennay Jr., P. Kaulfus, K. Weber, *Cell* **24**, 471 (1981).
27. J. E. Caldwell, S. G. Heiss, V. Mermall, J. A. Cooper, *Biochemistry* **28**, 8506 (1989).
28. A. E. Adams, J. R. Pringle, *J. Cell Biol.* **98**, 934 (1984).
29. R. P. Jansen, C. Dowzer, C. Michaelis, M. Galova, K. Nasmyth, *Cell* **84**, 687 (1996).
30. T. Kamei *et al.*, *J. Biol. Chem.* **273**, 28341 (1998).
31. K. Ozaki-Kuroda *et al.*, *Mol. Cell Biol.* **21**, 827 (2001).
32. D. H. Schott, R. N. Collins, A. Bretscher, *J. Cell Biol.* **156**, 35 (2002).

33. H. C. Yang, L. A. Pon, *Proc. Natl. Acad. Sci. U.S.A.* **99**, 751 (2002).
34. We thank M. Johnson and M. Strang for assistance with the electron microscopy; C. Koth, R. Adorn-Broza, B. Kus, and A. Edwards for advice on protein purification of GST-Bni1 fragments; A. Davidson for valuable time on his spectrofluorometer; H. Zhu and M. Joyce for technical assistance; and S. Kim, D. Schott, and M. Tyers for critical reading and assistance with the manuscript. Supported by NIH grants AI19883 (S.Z.), GH39066 (D.P. and A.B.), and GM59216 (E.B.); a National Cancer Institute of Can-

ada (NCIC) grant (C.B.); and an NCIC graduate student fellowship (M.E.).

**Supporting Online Material**  
[www.sciencemag.org/cgi/content/full/1072309/DC1](http://www.sciencemag.org/cgi/content/full/1072309/DC1)  
 Materials and Methods  
 Fig. S1  
 References S1 to S5

28 March 2002; accepted 27 May 2002  
 Published online 6 June 2002;  
 10.1126/science.1072309  
 Include this information when citing this paper.

# Modulation of Postendocytic Sorting of G Protein–Coupled Receptors

Jennifer L. Whistler,<sup>1\*</sup> Johan Enquist,<sup>2</sup> Aaron Marley,<sup>3</sup> Jamie Fong,<sup>1</sup> Fredrik Gladher,<sup>2</sup> Pamela Tsuruda,<sup>3</sup> Stephen R. Murray,<sup>3</sup> Mark von Zastrow<sup>3\*</sup>

Recycling of the mu opioid receptor to the plasma membrane after endocytosis promotes rapid resensitization of signal transduction, whereas targeting of the delta opioid receptor (DOR) to lysosomes causes proteolytic down-regulation. We identified a protein that binds preferentially to the cytoplasmic tail of the DOR as a candidate heterotrimeric GTP-binding protein (G protein)–coupled receptor-associated sorting protein (GASP). Disruption of the DOR-GASP interaction through receptor mutation or overexpression of a dominant negative fragment of GASP inhibited receptor trafficking to lysosomes and promoted recycling. The GASP family of proteins may modulate lysosomal sorting and functional down-regulation of a variety of G protein–coupled receptors.

Ligand-induced endocytosis contributes to the physiological regulation of a wide variety of signaling receptors. Many G protein–coupled receptors (GPCRs) are endocytosed by a mechanism involving receptor phosphorylation, interaction with nonvisual (beta-) arrestins, and concentration in clathrin-coated pits [reviewed in (1, 2)]. However, the functional consequences of GPCR endocytosis through this conserved cellular mechanism are diverse. Trafficking of internalized GPCRs by a rapid recycling pathway restores the complement of functional receptors in the plasma membrane and promotes resensitization of receptor-mediated signal transduction (1, 3, 4). In contrast, the sorting of internalized GPCRs to lysosomes promotes proteolytic down-regulation of receptors, leading to a prolonged attenuation of cellular signal transduction (3, 5, 6). Furthermore, the post-endocytic sorting of certain GPCRs can itself be regulated under physiological conditions (7).

Mu opioid receptors (MORs) and DORs

<sup>1</sup>Department of Neurology, Ernest Gallo Clinic and Research Center, University of California, San Francisco, Emeryville, CA 94608, USA. <sup>2</sup>Program in Molecular Medicine, University of Lund, Sweden. <sup>3</sup>Program in Cell Biology, Department of Psychiatry and Department of Cellular and Molecular Pharmacology, University of California, San Francisco, CA 94143, USA.

\*To whom correspondence should be addressed. E-mail: shoocz@itsa.ucsf.edu (J.L.W); zastrow@itsa.ucsf.edu (M.v.Z.)

are structurally homologous GPCRs that mediate the actions of endogenously produced opioid neuropeptides and exogenously administered opiate drugs. Both receptors are endocytosed via clathrin-coated pits after agonist-induced activation, phosphorylation, and association with cytoplasmic beta-arrestins (8, 9). However, previous studies suggest that endocytosis causes different effects on MOR as compared to DOR (6, 10–12). A FLAG epitope–tagged DOR [DOR-1 (13)] expressed in stably transfected human embryonic kidney (HEK) 293 cells (14) exhibited pronounced down-regulation within 3 hours of exposure to opioid peptide agonist, whereas FLAG-tagged MOR [MOR-1 (15)] expressed at similar levels did not down-regulate (Fig. 1A) (16). A biochemical assay that specifically measures the fate of surface-biotinylated receptors (12, 17, 18) indicated that DOR but not MOR was rapidly proteolyzed after agonist-induced endocytosis (Fig. 1B). Fluorescence microscopy indicated that exposure of cells to agonist for 90 min caused DORs to concentrate in membranes located in the perinuclear region of the cells, many of which colocalized with the late endosome and lysosome markers LAMP1 and LAMP2 (Fig. 1C) (19). In contrast, MOR was localized under these conditions in vesicles distributed throughout the cytoplasm that failed to colocalize substantially with LAMP1 and

Downloaded from www.sciencemag.org on January 29, 2007